AIMS Biophysics

AIMS Biophysics, 12(2): 197−219.
DOI: 10.3934/biophy.2025012
Received: 29 November 2024
Revised: 14 March 2025
Accepted: 03 April 2025
Published: 25 April 2025

http://www.aimspress.com/journal/biophysics

Research article

Evaluation of L-methioninase as a targeted anticancer therapy in ovarian cancer and glioblastoma

Abbas Abed Noor Al-Owaidi* and Mohammed Abdullah Jebor

Department of Biology, College of Sciences, University of Babylon, Babylon, Hillah, 51001, Iraq

* **Correspondence:** Email: alowaidiabbas47@gmail.com; Tel: +9647705713626.

Abstract: Background and objective: A characteristic feature of many cancer cells, including glioblastoma and ovarian carcinoma, is their reliance on exogenous methionine for tumor proliferation. L-methioninase, an enzyme that degrades methionine, is being investigated as a potential agent for specifically targeting methionine-dependent cancers by disrupting critical cellular pathways necessary for cancer cell survival. This study evaluated the cytotoxic effects of L-methioninase (L-Met) on the glioblastoma cell line A-172 and the ovarian carcinoma cell line SK-OV-3, focusing on cell survival, nuclear integrity, and metastatic potential. Methods: L-Met was purified and tested for activity across a 25–200 µg/mL concentration range. Cytotoxicity was assessed using MTT assays, which measured viable cell count (VCC), total nuclear intensity (TNI), cell membrane permeability (CMP), and matrix metalloproteinase (MMP) activity. IC_{50} values were determined using Dunnett's multiple comparisons test. Results: L-Met significantly decreased cell viability in a dose-dependent manner for both cell lines. In A-172 cells, 200 and 100 µg/mL doses substantially reduced VCC and induced nuclear damage. In SK-OV-3 cells, these doses similarly reduced VCC and inhibited MMP activity, suggesting metastasis suppression. The IC_{50} values indicate that cancer cells are more sensitive to L-methioninase treatment than normal cells. Conclusion: L-Met demonstrates significant cytotoxic effects against glioblastoma and ovarian cancer cells, primarily through the induction of DNA damage, disruption of cell membranes, and suppression of metastasis. These findings support the potential of L-Met as a therapeutic agent for methionine-dependent cancers.

Keywords: L-methioninase; ovarian cancer; glioblastoma; cell viability; cancer

1. Introduction

Methionine is a sulfur-containing essential amino acid that plays a crucial role in various biochemical processes, including protein synthesis, methylation reactions, and the synthesis of S-adenosylmethionine (SAM), a key methyl donor in cellular functions. Since the body cannot synthesize methionine, it must be obtained through the diet [1]. A notable feature of many tumor cells, including glioblastoma and ovarian carcinoma, is their reliance on an external supply of methionine, making dietary methionine restriction (MR) a promising strategy for cancer treatment. MR has been shown to inhibit the proliferation of certain cancer cell types, while normal cells remain unaffected, provided homocysteine is available [2]. In addition to suppressing cancer cell proliferation, MR has demonstrated the ability to enhance the effectiveness of chemotherapy and radiation therapy in animal models [3]. Methionine dependency is a widespread characteristic of most cancer cells, which cannot proliferate without methionine, even in the presence of its precursor, homocysteine [3].

Glioblastoma, one of the most aggressive brain tumors, remains largely resistant to conventional therapies [4]. The high methionine dependence of glioblastoma may contribute to its aggressive nature, as reflected in the tumor's heightened uptake of 11C-methionine during positron emission tomography (PET) scans. Under normal physiological conditions, homocysteine can be remethylated to produce methionine, which is vital for processes such as the formation of SAM [5]. The remethylation process is mediated by methionine synthase, which transfers a methyl group from 5-methyltetrahydrofolate to homocysteine in a vitamin B12-dependent reaction. This reaction is part of the folate cycle, primarily powered by one-carbon units derived from the mitochondrial folate cycle [6]. In addition to remethylation, methionine can be synthesized through the salvage pathway from methylthioadenosine, a by-product of polyamine production. Mutations in enzymes involved in the de novo or salvage pathways of methionine synthesis may lead to methionine dependence [6].

Ovarian cancer is a leading cause of gynecological cancer-related mortality, often diagnosed at advanced stages due to its asymptomatic nature in early phases. This cancer is characterized by rapid metastasis and resistance to standard therapies, underscoring the need for novel treatment strategies [7]. Recent research has highlighted that ovarian cancer cells, like many other cancer types, exhibit methionine dependency. This dependency is thought to support uncontrolled tumor cell proliferation, as methionine is required for essential cellular processes such as DNA replication and protein synthesis [8]. Additionally, ovarian cancer cells have been shown to exhibit alterations in the methionine metabolism pathway, resulting in an increased demand for methionine to sustain rapid cell division and tumor progression. Targeting methionine metabolism through dietary MR or enzyme-based therapies has emerged as a potential approach to inhibit the growth of ovarian cancer cells and improve the effectiveness of other treatments [8].

DNA methylation, an important epigenetic modification, involves adding a methyl group to the cytosine base of CpG dinucleotides, affecting approximately 70% of cytosine residues. Cancer is associated with global DNA hypomethylation and gene-specific hypermethylation [9]. Hypermethylation of CpG islands in promoter regions of tumor suppressor genes can lead to their silencing, contributing to tumorigenesis [10]. SAM, the universal methyl donor, is essential for the methylation of DNA, RNA, histones, and proteins, influencing gene expression and cellular functions [11]. The methylation of specific genes, such as *TFPI2*, *SEPT9*, *GSTP1*, and *MGMT*, has been linked to tumor progression or suppression. Notably, methylation is reversible, suggesting that MR could potentially alter DNA methylation patterns, influencing cancer development and progression [12].

In this context, one promising candidate for targeted anticancer therapy is L-methioninase (L-Met), an enzyme that catalyzes the degradation of methionine, an essential amino acid [4]. Methionine is crucial for protein synthesis, methylation reactions, and cellular metabolism. This enzyme plays a pivotal role in methionine degradation [13]. L-Met is a pyridoxal phosphate (PLP)-dependent enzyme that catalyzes methionine cleavage. L-Met has demonstrated effectiveness in methionine depletion both in vitro and in vivo [14]. This study investigates the effects of L-methioninase on ovarian cancer and glioblastoma cells, exploring its mechanisms of action in inhibiting cell survival and disrupting cell cycle progression.

2. Materials and methods

2.1. Sample selection

A total of 150 clinical samples were randomly obtained from patients with urinary tract infections, burns, sputum infections, wounds, and otitis media at Baghdad Hospital. The clinical samples were non-blood specimens (urine, burn wounds, sputum, wound exudates, and ear swabs). All samples were transferred under sterile and refrigerated settings. Every volunteer has given written informed permission. This research received ethical approval (DSM-10256) for scientific research from the Ministry of Health MOH and Ministry of Higher Education and Scientific Research MOHESR ethics committees in Iraq.

2.2. Isolation and identification of Pseudomonas aeruginosa

Samples were subsequently cultured in brain heart infusion broth and underwent general and differential culture procedures. Colonies of *P. aeruginosa* were detected using lactose non-fermenting MacConkey agar, cetrimide agar for pyocyanin and fluorescein synthesis, and the VITEK-2 system. Bacterial identification was additionally confirmed using biochemical assays, including oxidase, catalase, indole, citrate consumption, and urease production.

2.3. Preparation of buffer

The buffers employed to sustain a certain pH in the enzyme activity assay included potassium phosphate buffer (0.5 M, pH 7), Tris-HCl buffer (0.05 M, pH 7), and Tris-base buffer (0.1 M, pH 8 and 9). Additional solutions, comprising sodium chloride (0.25 M), sodium hydroxide (0.25 M), and hydrochloric acid (0.25 M), were formulated for purifying purposes.

2.4. Assay for L-Met activity

The Nesslerization method was employed to assess the activity of L-Met. The reaction mixture, comprising 1% L-methionine, 0.5 M potassium phosphate buffer at pH 7, PLP, and crude enzyme, was incubated at 30 °C for 1 h. The reaction was terminated using trichloroacetic acid, and the emitted ammonia was evaluated with Nessler's reagent. Enzyme-specific activity was quantified as micromoles of ammonia generated per minute per milligram of protein.

2.5. Isolation and purification of L-Met

2.5.1. Ammonium sulfate precipitation

The crude enzyme was incorporated into the ammonium sulfate at several concentrations: 30%, 40%, 50%, 60%, 70%, and 80%. The enzyme underwent centrifugation at 6,000 rpm for 6 h at 4 °C. The optimal saturation was determined to be 70%, at which point the enzyme exhibited maximal activity.

2.5.2. Dialysis

An enzyme precipitate was dialyzed using a dialysis tube (molecular weight cutoff 3,500 Da) against potassium phosphate buffer, pH 7, at 4 °C for 24 h.

2.6. Ion-exchange chromatography

Subsequent purification of the target was conducted utilizing Diethylaminoethyl (DEAE) cellulose resin. The enzyme solution was introduced to the DEAE-cellulose column and rinsed with phosphate buffer. Proteins were eluted using stepwise gradients of sodium chloride at concentrations of 0.1 and 1 M. Enzyme activity and protein content were evaluated for each fraction.

2.7. Gel filtration chromatography

Gel filtration chromatography with Sephadex G-150 was conducted in the final step. The enzyme was introduced to a pre-equilibrated column, and fractions were obtained. Protein concentration was assessed for each enzyme activity.

2.8. Enzyme characterization

2.8.1. Ideal pH and temperature

The optimal pH of L-Met was assessed using buffers with pH values ranging from 4 to 9, while thermal stability was examined across a temperature spectrum of 10 to 60 °C. Activities were assessed based on substrate degradation under each circumstance.

2.8.2. Kinetic parameters

The kinetic parameters of the enzyme, Km (Michaelis constant) and Vmax (maximum reaction velocity), were ascertained from Lineweaver–Burk plots utilizing activity at different substrate concentrations.

2.9. Cytotoxicity assessment

2.9.1. Cell line cultivation

The cytotoxicity of L-Met was evaluated on two cancer cell lines, A-172 (glioblastoma) and SK-OV-3 (ovary carcinoma). Cells were grown in RPMI-1640 media enriched with 10% fetal bovine serum, 100 IU/mL penicillin, and 100 µg/mL streptomycin.

2.9.2. MTT assay

Tumor cells were inoculated in a 96-well plate (1×10^4 to 1×10^6 cells/mL) and treated for 24 h with serial dilutions of the enzyme at concentrations between 25 and 400 µg/mL. MTT solution was introduced to each well post-incubation, followed by an additional incubation period of 4 h. The purple formazan crystals produced from the reduction were solubilized in a solution and detected at 575 nm with an ELISA reader. The IC_{50} was determined by the enzyme concentration that resulted in a 50% reduction in cell viability. Figure 1 illustrates the schematic representation of the study procedure.

Viable cell count (VCC) and total nuclear intensity (TNI): VCC refers to measuring the number of living cells present after treatment with L-methioninase. VCC was determined using an automated cell viability analyzer (Trypan Blue exclusion assay). The number of viable cells was quantified and correlated with MTT absorbance readings.

TNI refers to measuring nuclear damage caused by the enzyme, which can indicate DNA damage or apoptosis. TNI was assessed using DAPI nuclear staining followed by fluorescence microscopy or high-content imaging analysis. ImageJ (automated imaging software) was used to quantify nuclear fluorescence intensity, which provides insights into nuclear integrity and condensation (indicators of apoptosis).

2.10. Cell membrane permeability (CMP)

CMP was measured using propidium iodide (PI) staining to detect membrane-compromised (non-viable) cells. Flow cytometry was used to quantify PI uptake in treated vs. untreated cells.

2.11. Matrix metalloproteinase (MMP) activity

MMP activity was measured using a specific MMP fluorogenic substrate assay or gelatin zymography to assess enzyme activity in conditioned media.

2.12. Statistical analysis

Before conducting statistical analyses, the normality of data was assessed using the Shapiro–Wilk test. Data following normal distribution were analyzed using parametric tests, while non-parametric tests were subjected to non-normally distributed data. All data are expressed as the mean ± standard deviation (SD) or mean ± standard error of the mean (SEM), as appropriate. Graphs were generated to visualize trends and comparisons between different experimental conditions, with error bars representing the variability in the data.

To compare the effects of different experimental conditions (e.g., carbon sources, nitrogen sources, pH, temperature, incubation period) on L-Met activity, a one-way analysis of variance (ANOVA) was performed. When significant differences were detected ($p < 0.05$), post-hoc pairwise comparisons were conducted using Tukey's honestly significant difference (HSD) test to identify which specific groups differed from each other. Repeated measures ANOVA was used for experiments involving time-dependent changes in enzyme activity (e.g., optimum incubation period). Post-hoc analyses were performed where necessary to identify specific time points with significant differences.

The cytotoxicity effects of L-Met on cancer cell lines (A-172 and SK-OV-3) were evaluated by measuring the VCC, TNI, CMP, and MMP. VCC, TNI, and CMP data were analyzed using Dunnett's multiple comparisons test to compare treated groups with the control group. Statistical significance was considered when the adjusted p-value was less than 0.05.

All experiments' results were considered statistically significant if the p-value was less than 0.05. All statistical analyses were conducted utilizing GraphPad Prism 9.4 software.

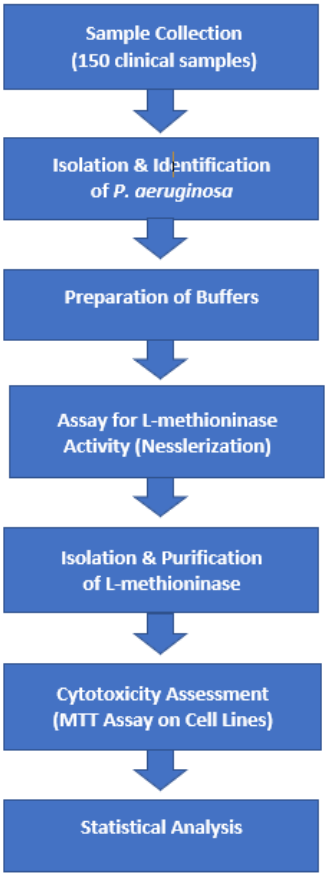

Figure 1. Schematic representation of the study procedure.

3. Results

3.1. Optimum conditions of bacterial isolates for L-Met enzyme production

3.1.1. Optimum carbon sources

To determine the optimal carbon source for the production of L-Met by *Pseudomonas aeruginosa*, various carbon sources, namely glucose, sucrose, maltose, xylose, and galactose, were tested as sole energy and carbon sources. The specific activity of the enzyme [units per milliliter (U/mL) protein] in cultures grown with different carbon sources is presented in Figure 2. Sucrose was identified as the most effective carbon source for enzyme production, yielding the highest specific activity of 1.2 U/mg protein. In contrast, maltose had the lowest enzyme activity among the carbon sources tested, with a specific activity of 0.25 U/mg protein. Xylose showed a moderate increase in enzyme activity, with a specific activity of 0.4 U/mg protein, higher than that observed for maltose. Glucose, with a specific activity of 0.45 U/mg protein, exhibited better enzyme production than xylose. Finally, galactose significantly enhanced enzyme activity, achieving a specific activity of 1.0 U/mg protein.

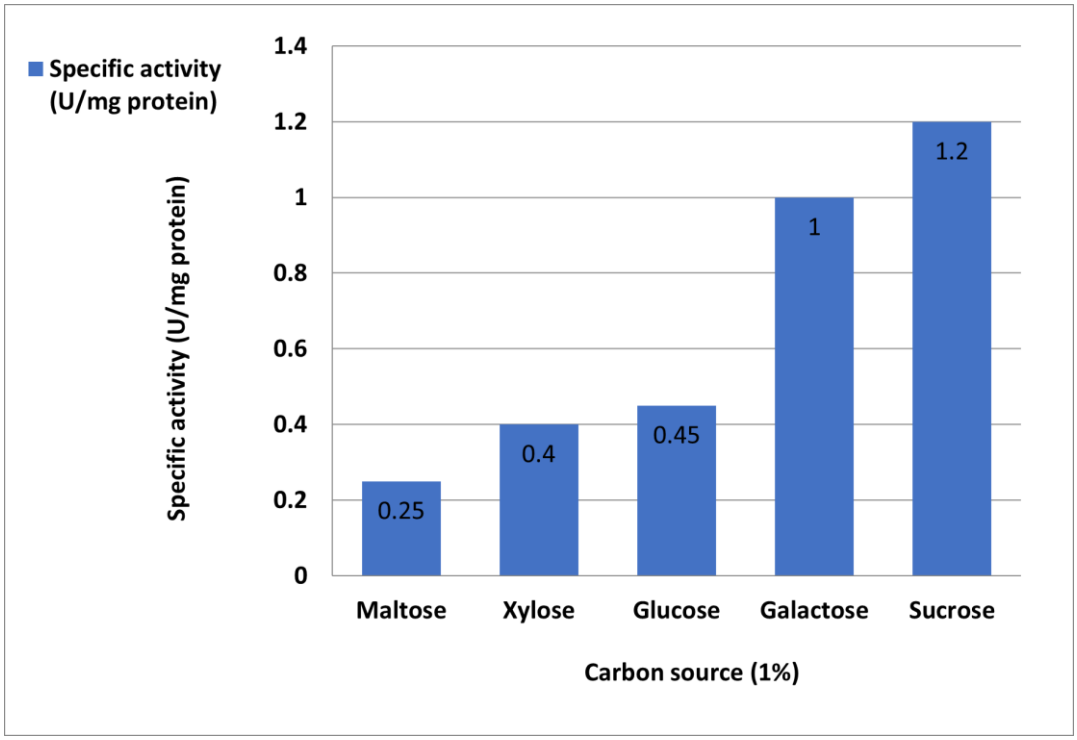

Figure 2. Optimal carbon source for L-Met production from *Pseudomonas aeruginosa* after incubation at 37 °C for 48 h.

3.1.2. Optimum nitrogen sources

To identify the optimal nitrogen source for L-Met production by *Pseudomonas aeruginosa*, various nitrogen sources, namely tryptone, peptone, NH_4Cl, yeast extract, and casein, were evaluated. Each nitrogen source was added to the medium at a concentration of 1% (w/v) to assess its impact on

enzyme synthesis.

Figure 3 illustrates the specific activity of L-Met when cultivated with different nitrogen sources, expressed as U/mg protein. Among the tested nitrogen sources, tryptone was the most effective, yielding the highest specific activity of 2.6 U/mg protein. In comparison, NH_4Cl resulted in a lower specific activity of 0.8 U/mg protein, indicating reduced enzyme production relative to other nitrogen sources.

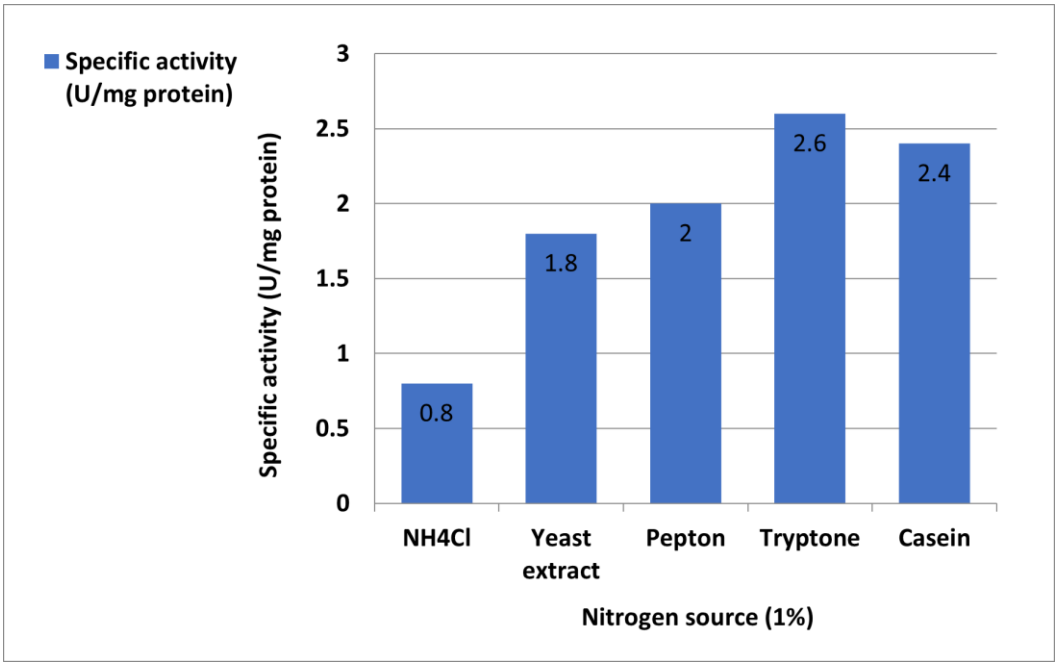

Figure 3. Optimal nitrogen source for L-Met production from *Pseudomonas aeruginosa* A6 after incubation at 37 °C for 48 h.

3.1.3. Optimum temperature

From 10 to 60 °C, temperature stability was noted. Until 37 °C, enzyme activity rose with temperature, peaking at 1.5 U/mL. Enzyme activity decreased with increasing temperature, reaching 0.9 U/mL at 42 °C and 0.5 U/mL at 47 °C, suggesting that enzyme performance is diminished at higher temperatures. The enzyme's specific activity also increased as the temperature rose, peaking at 37 °C at 2.7 U/mg protein. However, specific activity dropped to 0.9 U/mg protein at 42 °C, indicating that enzyme efficiency decreases with increasing temperature (Figure 4).

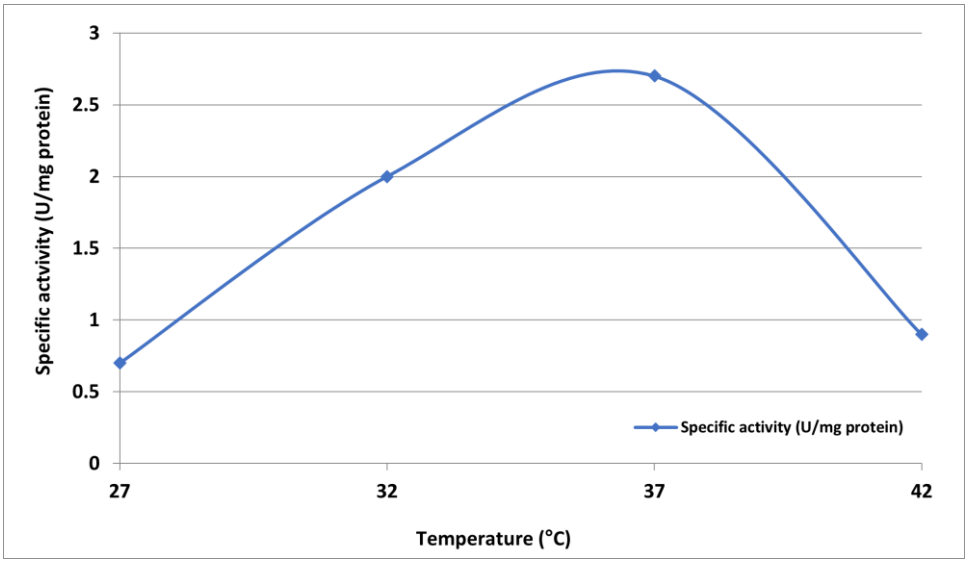

Figure 4. Effect of temperature on the specific activity of L-Met enzyme. L-Met specific activity (U/mg protein) was measured at temperatures ranging from 10 to 60 °C.

3.1.4. Optimum pH

The optimal pH range for L-Met activity was found to be between pH 4 and pH 9. The enzyme exhibited the highest activity at pH 7, with a noticeable decline at both more acidic and alkaline pH values. Moreover, the enzyme's stability and activity were greatest at pH 7 and pH 8, while activity significantly decreased at both highly acidic and highly alkaline pH levels (Figure 5).

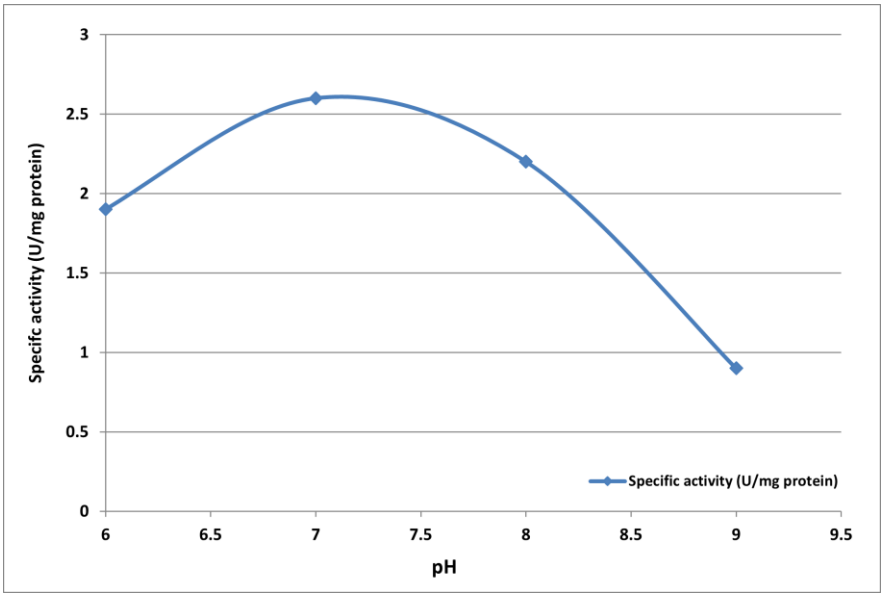

Figure 5. Optimal pH for L-Met production from *Pseudomonas aeruginosa* A6 after incubation at 37 °C for 48 h. Enzyme activity was measured at pH values ranging from 4 to 9.

3.1.5. Optimal incubation period

Over 48 h, the enzyme's specific activity rose to a maximum of 3.3 U/mg protein. Nevertheless, after 72 h, the specific activity dropped to 2.5 U/mg protein, suggesting a reduction in enzyme efficiency with extended incubation (Figure 6).

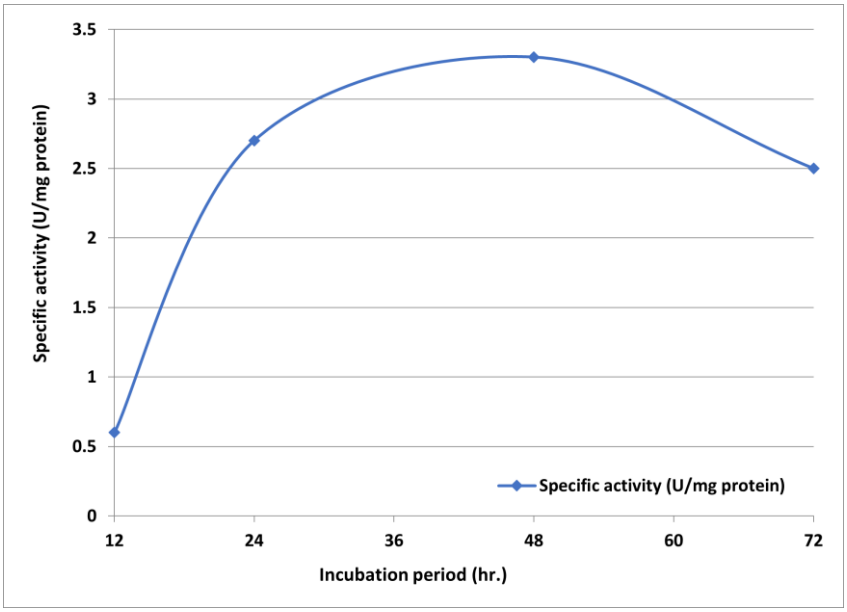

Figure 6. The optimal incubation period for *P. aeruginosa* producing L-Met at 37 °C. L-Met-specific activity (U/mg protein) was measured over 72 h.

3.2. Purification of L-met from P. aeruginosa

Three purification steps were employed to isolate the L-Met produced by *P. aeruginosa*. The initial phase involved the precipitation of L-methioninase using ammonium sulfate. A precipitation range of 30%–80% ammonium sulfate saturation was applied to the crude enzyme solution. The optimal condition for preserving enzyme activity was found at 70% ammonium sulfate saturation, which resulted in the highest enzyme activity (4.5 U/mL) and specific activity (11.2 U/mg protein) (Table 1).

Table 1. Enzyme activity and specific activity of L-Met at different ammonium sulfate saturation levels.

Ammonium sulfate (%)	Activity (U/mL)
30	0.9
40	1.5
50	2
60	4
70	4.5
80	3.8

3.3. Ion-exchange chromatography (IEC)

To further purify the enzyme, DEAE-cellulose resin was employed. The enzyme fractions were eluted using a sodium chloride gradient (ranging from 0.1 to 1 M), and both protein content and activity were assessed. IEC separates ionizable molecules based on differences in their charge properties. The collected fractions were analyzed by measuring their optical density (OD) at 280 nm using a spectrophotometer.

A distinct protein peak appeared during the washing step, where a potassium phosphate buffer was used to elute positively charged proteins. The washing continued until the OD values reached zero, indicating the complete removal of positively charged proteins from the column. A second peak was obtained during the elution phase, where a gradient of sodium chloride concentrations was applied to release the negatively charged proteins bound to the column.

Fractions 59–66 contained the majority of L-Met activity. These fractions exhibited a purification fold of 2.6, with an overall yield of 48%, and their specific activity was determined to be 10.7 U/mg protein (Figure 7).

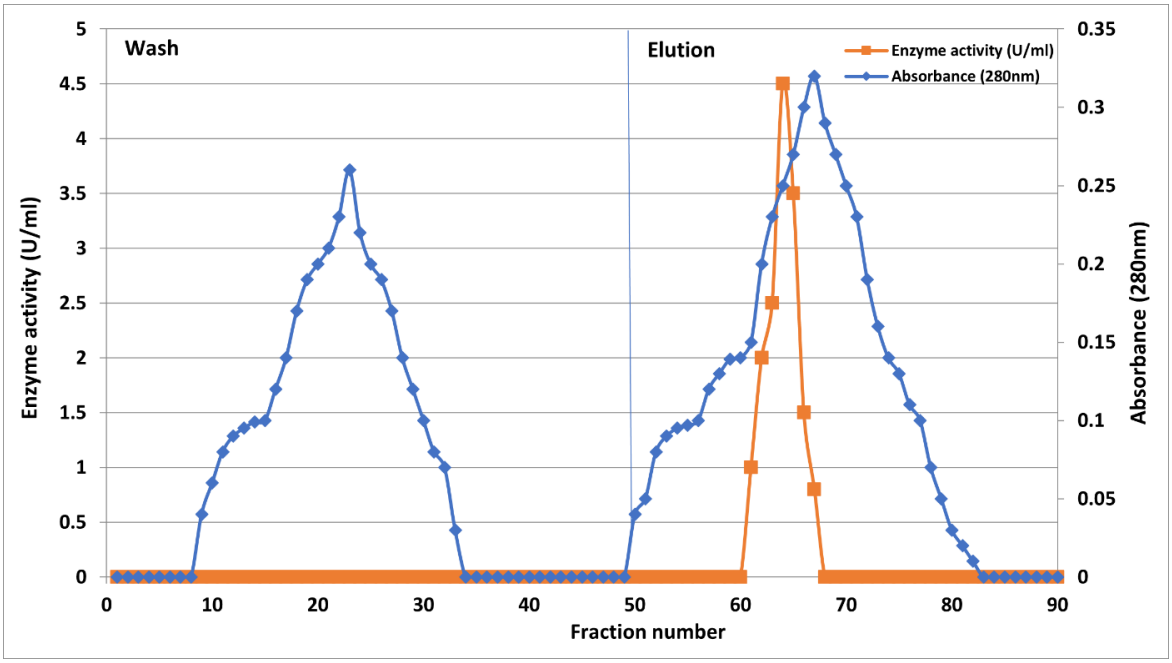

Figure 7. Ion-exchange chromatography of L-Met enzyme using DEAE-cellulose resin. Protein elution was performed using a sodium chloride gradient (0.1–1 M).

3.4. Gel filtration chromatography using Sephadex G-150

The final purification step involved Sephadex G-150 gel filtration, which successfully isolated L-methioninase. The fractions obtained during this step were analyzed for protein concentration and enzyme activity (Figure 8). Gel filtration with Sephadex G-150 resulted in a significant increase in the enzyme's specific activity, reaching 16.6 U/mg, along with a 4.6-fold improvement in purity. However, the recovery yield from this step was slightly lower at 45% compared to other purification methods (Table 2).

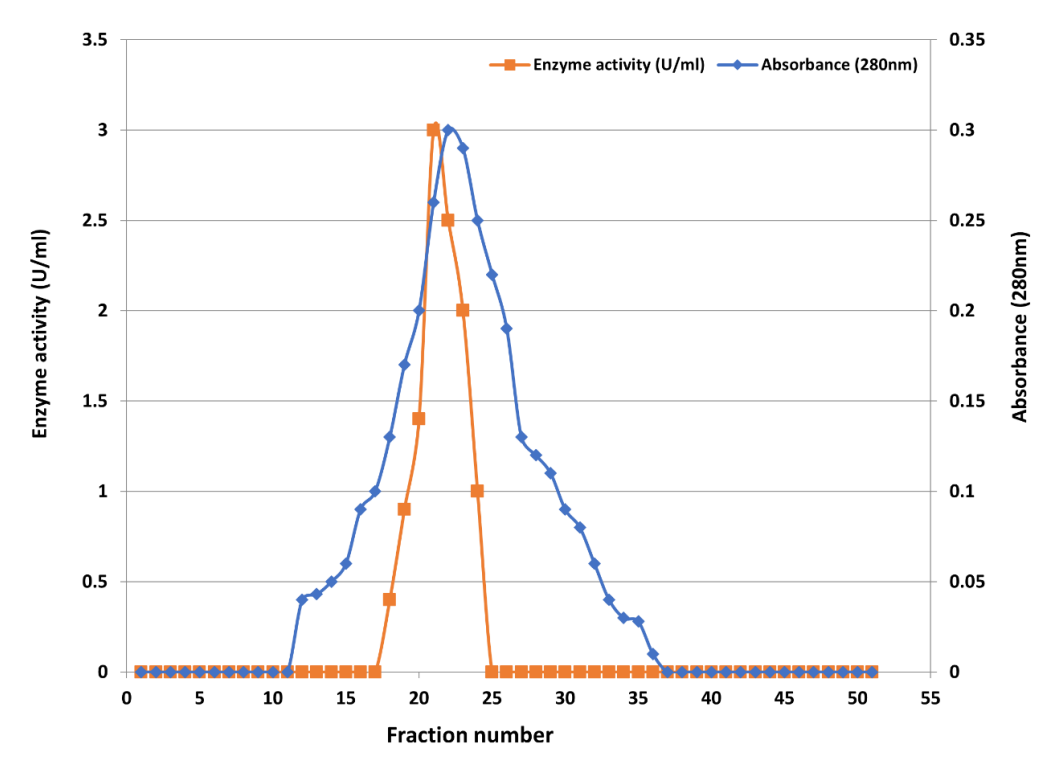

Figure 8. Gel filtration chromatography of L-Met enzyme using Sephadex G-150. Protein concentration and enzyme activity were measured for each fraction.

3.5. Characterization of purified L-Met enzyme

3.5.1. Effect of PH on enzyme activity and stability

Table 2. Purification procedures for L-Met production from *Pseudomonas aeruginosa*.

Purification step	Volume (mL)	Enzyme activity (U/mL)	Protein concentration (mg/mL)	Specific activity (U/mg)	Total activity (U)	Purification (folds)	Yield (%)
Crude enzyme	70	1	0.3	3.3	70	1	100
Ammonium sulfate precipitation (70%)	11	4.5	0.4	11.2	49.5	3.4	70.7
DEAE-cellulose	21	2.2	0.1	22	46.2	6.6	66
Sephadex-G150	21	1.5	0.09	16.6	31.5	5	45

The relationship between pH and enzyme activity, measured in U/mL, is illustrated in Figure 9. The enzyme demonstrated optimal activity at a pH of approximately 7, with a maximum enzyme

activity of 1.5 U/mL. Activity declined under both more acidic (pH 5) and more basic (pH 9) conditions. Furthermore, enzyme activity gradually decreased at higher alkaline (pH 9 and 10) and acidic (pH 5) pH values, with optimal structural stability occurring at pH 7 and 8.

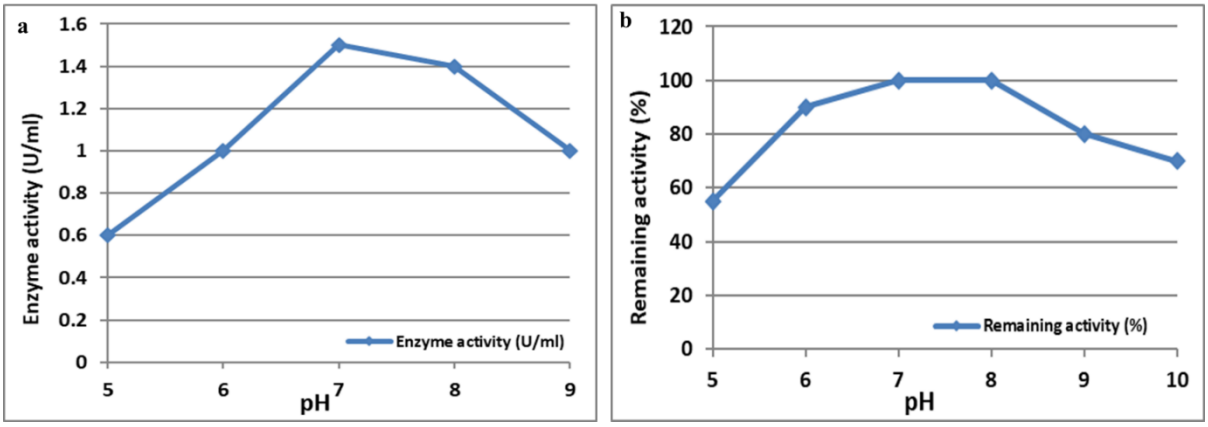

Figure 9. (a) Effect of different pH values on enzyme-specific activity. L-Met-specific activity (U/mL) was measured at pH values from 5 to 10. (b) Effect of different pH on the enzyme structure stability. Enzyme stability was assessed as residual activity (%).

3.5.2. Effect of temperature on enzyme activity and stability

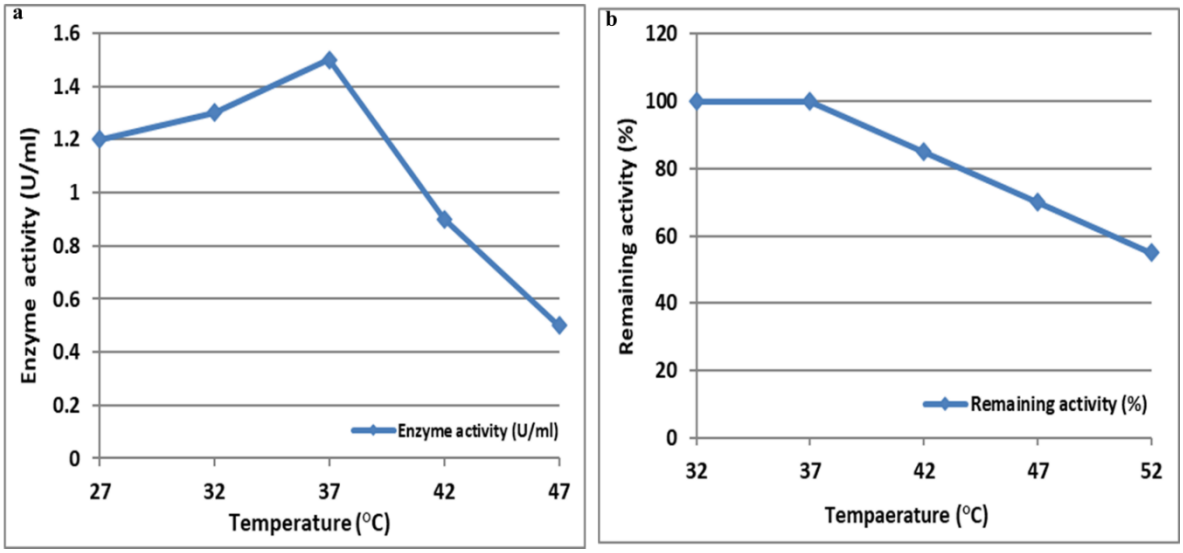

Figure 10. (a) Optimum temperature for enzyme-specific activity. L-Met-specific activity (U/mL) was measured at temperatures from 32 to 47 °C. (b) Optimum temperature for enzyme structure stability. Enzyme stability was assessed as residual activity (%).

The relationship between temperature and enzyme activity, expressed in U/mL, is shown in Figure 10. The enzyme exhibited optimal activity at 37 °C, with specific activity reaching its peak at this temperature and declining at both lower and higher temperatures. The percentage of residual enzyme

activity, as illustrated in Figure 10, indicates the enzyme's structural stability across different temperatures. Maximum structural stability was maintained at 32 °C and 37 °C. However, as the temperature exceeded 37 °C, enzyme stability decreased, with significant reductions in activity observed at temperatures above 42 °C. This suggests that the enzyme loses its structural integrity at elevated temperatures, with the enzyme being most stable between 32 and 37 °C.

3.6. Evaluation of purity via polyacrylamide gel electrophoresis (PAGE)

Polyacrylamide gel electrophoresis (PAGE) was employed to assess the purity of L-Met isolated from *P. aeruginosa*. After the gel filtration step, the protein profile analysis revealed a single band, indicating that the enzyme was highly purified. The molecular weight of the purified L-Met was approximately 55 kDa.

3.7. Effect of ionic factors on L-met activity

The activity of L-Met was measured using the Nesslerization method. The reaction mixture, containing 1% L-Met, potassium phosphate buffer, pyridoxal phosphate (PLP), and crude enzyme, was incubated at 30 °C for 1 h. After the reaction was terminated, the Nessler reagent was added to assess ammonia release. The enzyme's specific activity was quantified in micromoles of ammonia produced per minute per milligram of protein.

Table 3 displays the residual activity of L-Met after exposure to various ionic compounds at a concentration of 5 mM. The control enzyme retained 100% activity. Exposure to $NaNO_3$ and $CuCl_2$ reduced enzyme activity to 70%, indicating mild inhibition. In contrast, $CaCl_2$ resulted in 90% residual activity, suggesting only mild inhibition. $MnCl_2$ and KCl did not affect enzyme activity, maintaining 100% residual activity. These results indicate that certain salts, such as $MnCl_2$ and KCl, do not inhibit L-Met activity, whereas others, such as $NaNO_3$ and $CuCl_2$, have a mild inhibitory effect.

Table 3. Effect of various reagents on the activity of L-Met enzyme.

Reagent	Concentration (mM)	Remaining activity (%)
Control (enzyme)		100
$NaNO_3$	5	70
$CaCl_2$	5	90
$CuCl_2$	5	70
$MnCl_2$	5	100
KCl	5	100

3.8. L-Met cytotoxicity effect on cancer cell lines

In the present work, we assessed the cytotoxic effects of the L-Met on A-172 (glioblastoma) and SK-OV-3 (ovary carcinoma) cell lines. The main parameters during this test included VCC, TNI, CMP, and MMP, all demonstrating the action of L-methioninase on cellular viability, structural integrity, and metastatic potential.

A-172 glioblastoma cells exhibited a dose-related response for VCC. Specifically, an agent concentration at 200 μg/mL resulted in a significantly lower viable cell count than cells subjected to

the vehicle control (mean diff. = 3749, adjusted p = 0.0037), showing its effective cytotoxic action. Although the lower doses, such as 100 µg/mL, also experienced a drop in VCC, the effect was less impressive but still significant, with a p = 0.0075; higher concentrations were more effective for killing the glioblastoma cells. The changes in VCC in A-172 at 50 and 25 µg/mL were non-significant. L-Met showed a dose-dependent cytotoxic effect on both cell lines. The IC_{50} value for L-Met was 100.9 µg/mL for A172 cells and 214.0 µg/mL for WRL68 cells (Figure 11).

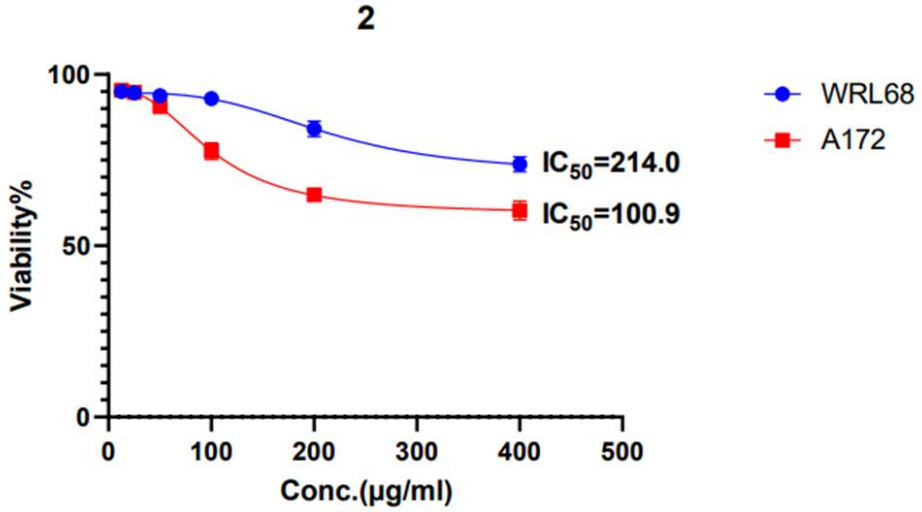

Figure 11. Dose-response curves for L-Met therapy in the normal cell line WRL68 and the glioma cell line A172. Cell viability was evaluated after 24 h of exposure to different concentrations of L-Met (25–500 µg/mL). Error bars represent standard deviations from trials completed in triplicate.

As shown in Table 4, at 200 µg/mL, the TNI significantly decreased (mean diff. = 3048, adjusted p = 0.0016), an excellent indication of extensive nuclear damage. This may point to the fact that the agent induces DNA damage, or nuclear functions interfere with the agent and trigger programmed cell death or apoptosis. Other concentrations, at 100, 50, and 25 µg/mL, lowered the TNI, but not as markedly.

As Table 5 depicts, the agent significantly increased membrane permeability at 200 and 100 µg/mL, with a mean diff. of 2757 and 1959 and an adjusted p of 0.0137 and 0.0465, respectively, indicating that at higher doses, the agent impairs the integrity of the membrane of glioblastoma cells. This is further supported by findings in the 50 and 25 µg/mL results, which showed no significant membrane disruption, showing this to be dose dependent.

Table 4. Dunnett's multiple comparisons test results for TNI in A-172.

Dunnett's multiple comparisons test	Mean 1	Mean 2	Mean diff.	95% CI of diff.	Below threshold?	Summary	Adjusted p-value	SE of diff.	n1	n2	q	DF
Untreated vs. 200 μg/mL	4401	1353	3048	2523–3967	Yes	**	0.0016	249.4	2	2	6.654	5
Untreated vs. 100 μg/mL	4401	1890	2511	1871–3478	No	ns	0.6034	300.2	2	2	8.070	5
Untreated vs. 50 μg/mL	4401	2997	1404	907–2301	No	ns	0.7032	233.0	2	2	6.996	5
Untreated vs. 25 μg/mL	4401	3240	1161	409–1659	No	ns	0.7608	339.9	2	2	5.859	5

DF stands for degrees of freedom, a key value in statistical tests that helps determine the appropriate critical value for the test statistics. **n1** and **n2** represent the sample sizes for the comparison groups. Specifically, **n1** is the number of samples in the first group (untreated), and **n2** is the number of samples in the second group (treated with a specific concentration).

Table 5. Dunnett's multiple comparisons test results for CMP in A-172.

Dunnett's multiple comparisons test	Mean 1	Mean 2	Mean diff.	95% CI of diff.	Below threshold?	Summary	Adjusted p-value	SE of diff.	n1	n2	q	DF
Untreated vs. 200 μg/mL	3994	1237	2757	2041–3179	Yes	**	0.0137	311.4	2	2	9.062	5
Untreated vs. 100 μg/mL	3994	2035	1959	1253–2608	Yes	**	0.0465	244.7	2	2	5.289	5
Untreated vs. 50 μg/mL	3994	2827	1167	719–1912	No	ns	0.8378	228.3	2	2	6.386	5
Untreated vs. 25 μg/mL	3994	2535	1459	813–2179	No	ns	0.9735	254.7	2	2	5.158	5

As suggested by Table 6, treatment at 200 μg/mL considerably reduced MMP activities (mean diff. = 2827, adjusted p = 0.01098). This shows that such an agent can reduce the metastatic potential of A-172 cells by reducing their ability to degrade the extracellular matrix. Low doses did not demonstrate a significant effect, and higher concentrations of L-methioninase may be needed for the anti-metastatic activity.

Table 6. Dunnett's multiple comparisons test results for MMP in A-172.

Dunnett's multiple comparisons test	Mean 1	Mean 2	Mean diff.	95% CI of diff.	Below threshold?	Summary	Adjusted p-value	SE of diff.	n1	n2	q	DF
Untreated vs. 200 µg/mL	4822	1995	2827	2186–3294	Yes	**	0.01098	266.1	2	2	9.036	5
Untreated vs. 100 µg/mL	4822	3865	957	287–1601	No	ns	0.8802	360.7	2	2	7.717	5
Untreated vs. 50 µg/mL	4822	4005	817	37–1223	No	ns	0.8313	383.0	2	2	6.970	5
Untreated vs. 25 µg/mL	4822	3558	1264	659–2047	No	ns	0.8937	347.1	2	2	5.197	5

The VCC results against SK-OV-3 cells indicate that there is a significant decrease in the number of surviving cells at both 200 and 100 µg/mL (mean diff. = 2411, adjusted p = 0.0080; and mean diff. = 2848, adjusted p = 0.0076, respectively). This indicates that in ovary carcinoma, L-Met is potent for destroying glioblastoma cells, requiring higher doses to achieve this goal: the IC_{50} for SK-OV-3 cells was 105.5 µg/mL, compared to 214.0 µg/mL for WRL68 cells (Figure 12).

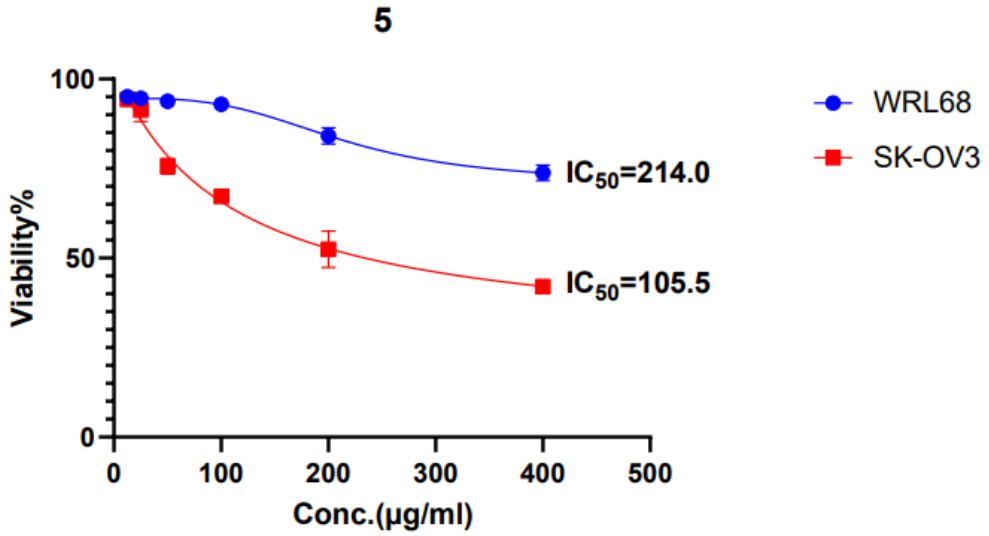

Figure 12. Dose-response curves for L-Met therapy in the normal cell line WRL68 and the ovarian line SK-OV-3. Cell viability was evaluated after 24 h of exposure to different concentrations of L-Met (25–500 µg/mL). Error bars represent standard deviations from trials completed in triplicate.

L-Met significantly decreased TNI at 200 µg/mL vs. control, as shown in Table 7 (mean diff. = 3257, adjusted p = 0.0364), with L-Met inducing extensive nuclear damage in SK-OV-3 cells at this concentration. Curiously, 50 and 25 µg/mL resulted in higher TNI reductions than 100 µg/mL (Table 7).

Table 7. Dunnett's multiple comparisons test results for TNI in SK-OV-3.

Dunnett's multiple comparisons test	Mean 1	Mean 2	Mean diff.	95% CI of diff.	Below threshold?	Summary	Adjusted p-value	SE of diff.	n1	n2	q	DF
Untreated vs. 200 µg/mL	3376	119	3257	2496–3770	Yes		0.0364	369.5	2	2	9.362	5
Untreated vs. 100 µg/mL	3376	1705	1671	959–2650	No	ns	0.1588	240.6	2	2	6.695	5
Untreated vs. 50 µg/mL	3376	996	2380	1753–3258	No	ns	0.9426	242.5	2	2	7.871	5
Untreated vs. 25 µg/mL	3376	691	2685	1942–3221	No	ns	0.7353	331.7	2	2	5.478	5

Table 8 shows significant decreases in CMP on SK-OV-3 cells at 200 and 100 µg/mL (mean diff. = 3168 and 2284, and adjusted p = 0.0090 and 0.0051, respectively), reducing membrane disruption and, thus, cytotoxicity. Similarly, 50 and 25 µg/mL showed a strong effect, though to a lesser degree.

Table 8. Dunnett's multiple comparisons test results for CMP in SK-OV-3.

Dunnett's multiple comparisons test	Mean 1	Mean 2	Mean diff.	95% CI of diff.	Below threshold?	Summary	Adjusted p-value	SE of diff.	n1	n2	q	DF
Untreated vs. 200 µg/mL	4467	1299	3168	2723–3953	Yes		0.0090	276.3	2	2	8.002	5
Untreated vs. 100 µg/mL	4467	2183	2284	1754–3033	Yes		0.0051	288.2	2	2	8.109	5
Untreated vs. 50 µg/mL	4467	3397	1070	420–1640	No	ns	0.1716	243.4	2	2	8.144	5
Untreated vs. 25 µg/mL	4467	3197	1270	671–2062	No	ns	0.1253	247.6	2	2	9.573	5

As represented in Table 9, the MMP activity significantly declined at 200 µg/mL in SK-OV-3 cells, with a mean difference of 1603 and an adjusted p-value of 0.0188. Lower doses revealed variable activities, which means they were dose dependent.

Table 9. Dunnett's multiple comparisons test results for MMP in SK-OV-3.

Dunnett's multiple comparisons test	Mean 1	Mean 2	Mean diff.	95% CI of diff.	Below threshold?	Summary	Adjusted p-value	SE of diff.	n1	n2	q	DF
Untreated vs. 200 µg/mL	4755	3152	1603	1077–2436	Yes		0.0188	351.7	2	2	7.435	5
Untreated vs. 100 µg/mL	4755	3190	1565	1114–2199	No	ns	0.1210	272.3	2	2	8.318	5
Untreated vs. 50 µg/mL	4755	4008	747	88–1602	No	ns	0.5058	354.4	2	2	8.204	5
Untreated vs. 25 µg/mL	4755	3746	1009	587–1933	No	ns	0.7216	366.6	2	2	8.434	5

4. Discussion

Some bacterial strains, including *P. aeruginosa*, produce L-Met, an enzyme that degrades methionine into methanethiol, α-ketobutyrate, and ammonia. This enzyme plays a role in bacterial metabolism and pathogenesis by modulating sulfur metabolism and influencing host immune responses. Understanding the production of L-methioninase in *P. aeruginosa* isolates is crucial, as it could have implications for bacterial virulence, antibiotic resistance, and potential therapeutic targeting [15].

The research indicated that L-Met showed significant cytotoxicity against the A-172 and SK-OV-3 cell lines. A definitive dose-response relationship was established, suggesting that elevated concentrations of L-Met markedly reduced cancer cell viability, induced substantial nuclear damage, and compromised cell membrane integrity in both malignancies. The evident reliance of numerous human malignancies on exogenous methionine has prompted suggestions that MR or depletion could offer a method to impede or eradicate human tumors.

In 2024, Kholmurodov and Jurayev demonstrated that a diet without methionine, leucine, or valine inhibited the formation of Walker tumors implanted in the flanks of Sprague-Dawley rats [16]. Subsequent animal studies have demonstrated other health advantages of diminished methionine intake, including lower obesity, enhanced insulin sensitivity, decreased inflammation and oxidative stress, and prolonged lifespan. The findings indicate that dietary MR may benefit cancer patients [9]. In human investigations, the depletion of dietary methionine has exhibited a synergistic effect with 5-fluorouracil (5FU) in patients who have advanced stomach cancer. A phase 1 investigation with eight human individuals demonstrated a reduction in plasma methionine levels from 21 ± 7.3 to 9 ± 4 µM over two weeks on a methionine-free diet [17].

In 2007, Thivat et al. investigated the efficacy of chloroethylnitrosurea and cystemustine, in conjunction with a methionine-free diet, in 22 patients diagnosed with melanoma and glioblastoma. These studies and others suggest that dietary limitation of methionine, in conjunction with cytotoxic treatment, may impede the advancement of some human malignancies. However, the clinical application

of dietary MR presents significant challenges, especially in glioblastoma, due to the blood–brain barrier (BBB), which limits the ability of nutritional changes to reduce methionine levels in the brain effectively [18]. Locasale et al. analyzed metabolites in cerebrospinal fluid from glioma patients and controls, further highlighting the challenges of systemic MR in brain cancers [19].

Our study aligns with these earlier findings, where L-Met was shown to significantly reduce cell viability in glioblastoma (A-172) and ovarian carcinoma (SK-OV-3) cell lines. The reduction in VCC observed at higher concentrations of L-Met, particularly at 200 and 100 μg/mL, suggests that methionine depletion impedes tumor growth by inducing cell death. This is consistent with the results of dietary MR, which has been demonstrated to inhibit tumor growth in preclinical models [16,18]. Our findings indicate that L-Met induces significant reductions in cancer cell viability, nuclear damage, and disruption of cellular integrity, similar to the effects of dietary MR, which stresses methionine-dependent metabolic pathways in tumor cells, potentially leading to apoptosis.

The clinical significance of L-Met lies in its ability to selectively disrupt methionine metabolism in cancer cells, a critical pathway for the growth and survival of many tumors. As a result, L-Met can reduce the reliance of tumors on methionine, effectively "starving" them without causing widespread nutrient depletion in healthy tissues. This targeted approach is particularly beneficial in cases where dietary MR may not be feasible due to the limitations imposed by the BBB in brain tumors like glioblastoma [20].

Recent studies, such as the work by Lu et al. (2019), have identified that LAT1, a transporter protein, plays a critical role in glioma cells by facilitating methionine uptake across the BBB. This overexpression of LAT1 in gliomas has been correlated with tumor progression and increased microvascular density. LAT1-mediated methionine uptake contributes to methionine dependency in glioma cells, which our results also support, as the SK-OV-3 cells exhibited substantial reductions in VCC and nuclear damage, even in the presence of the LAT1 transporter [21].

Our findings indicate that L-Met could potentially overcome this issue by directly targeting methionine metabolism in tumors, bypassing the need for dietary MR or systemic approaches that are hindered by the BBB. This could be an important therapeutic advantage, as it would allow for localized methionine depletion in glioblastoma and other brain tumors without the side effects associated with dietary restriction or systemic therapies. Moreover, recent pharmacological studies have focused on creating inhibitors targeting methionine metabolic pathways or employing recombinant L-Met as part of tumor-eradicating therapies [22,23]. Our study also supports these findings, showing that L-Met could work synergistically with existing cancer therapies, such as chemotherapy agents, to enhance treatment efficacy. Previous studies have demonstrated that methionine depletion, in combination with cytotoxic treatments like 5FU, enhances tumor response [18], and our data indicate similar synergy when using L-Met in combination with other therapeutic agents.

Aligned with our findings, Kubotaet al. demonstrated that L-Met has emerged as a promising therapeutic agent in ovarian cancer treatment due to its ability to selectively target cancer cells while minimizing toxicity to healthy tissues [24]. L-Met selectively targets and eliminates cancer stem cells (CSCs) in ovarian cancer by exploiting the unique metabolic vulnerabilities of these cells. Ovarian cancer stem cells (OCSCs) exhibit a high dependence on methionine metabolism, which is crucial for their survival and proliferation. By inhibiting methionine utilization, L-Met disrupts the metabolic pathways that sustain OCSCs, leading to their selective elimination [25].

While dietary MR has shown promise, it presents several challenges, particularly in advanced cancer patients. One major issue is the risk of systemic malnutrition, which can exacerbate cachexia

and decrease overall survival [26]. As patients with cancer already experience nutrient deficiencies and metabolic imbalances, further restriction of essential amino acids like methionine could result in harmful side effects, such as weakened immune response and muscle wasting [27].

In contrast, L-Met offers a more targeted approach by specifically depleting methionine within the tumor without the systemic side effects associated with dietary MR. The enzyme's ability to be administered directly to the tumor site minimizes the risk of global nutrient deficiencies while effectively impairing the growth and survival of tumors. This makes L-Met a promising candidate for targeted cancer therapy, particularly when systemic dietary MR is impractical or dangerous [25].

A limitation of the current study is that only a limited number of cell lines per cancer type were tested. Future studies should consider expanding the range of cell lines to better understand the generalizability of the findings across different models. Specifically, for glioblastoma, it is important to note that several resistance mechanisms are differently regulated between various cell lines, which may lead to potential misinterpretations.

5. Conclusions

L-Met demonstrates significant cytotoxicity toward glioblastoma and ovarian cancer cells by DNA damage, membrane rupture, and metastasis inhibition; hence, it is a potential treatment for methionine-dependent malignancies. The results of this investigation validate the significant cytotoxic efficacy of L-Met against glioblastoma and ovarian cancer cell lines. Stimulating cell death by processes such as DNA damage, membrane permeability disruption, and metastasis suppression validates the enzyme's application as a therapeutic agent. L-Met exhibited dose-dependent cytotoxicity; increased dosage corresponded with enhanced efficacy in diminishing cell viability by undermining cellular integrity. The findings indicate that targeting tumor methionine metabolism by L-Met is a highly promising strategy for cancer treatment, especially for cancer types exhibiting methionine reliance, such as glioblastoma and ovarian carcinoma. Additional research is required to determine this enzyme's clinical relevance and explore its efficacy in conjunction with other therapeutic strategies.

Use of generative-AI tools declaration

The authors declare they have not used Artificial Intelligence (AI) tools in the creation of this article.

Acknowledgments

My thanks and appreciation also to Assist. Prof. Dr. Yasir Haider Al-Mawlah DNA Research Center, University of Babylon, for supporting me and providing me with greater assistance, through his worthwhile comments as I work on my thesis.

Thanks, and appreciation to all the faculty members of the Department of Biology, College of Sciences, University of Babylon, as many of them guided me during the investigation of my thesis.

Conflict of interest

The authors declare no conflict of interest.

Author contributions

Conception and design of study: Abbas Abed Noor Al-Owaidi and Mohammed Abdullah Jebor. Drafting the manuscript: Abbas Abed Noor Al-Owaidi. Analysis and/or interpretation of data: Mohammed Abdullah Jebor.

References

1. Tassinari V, Jia W, Chen WL, et al. (2024) The methionine cycle and its cancer implications. *Oncogene* 43: 3483−3488. https://doi.org/10.1038/s41388-024-03122-0
2. Wanders D, Hobson K, Ji X (2020) Methionine restriction and cancer biology. *Nutrients* 12: 684. https://doi.org/10.3390/nu12030684
3. Gao X, Sanderson SM, Dai Z, et al. (2019) Dietary methionine influences therapy in mouse cancer models and alters human metabolism. *Nature* 572: 397−401. https://doi.org/10.1038/s41586-019-1437-3
4. Wu W, Klockow JL, Zhang M, et al. (2021) Glioblastoma multiforme (GBM): an overview of current therapies and mechanisms of resistance. *Pharmacol Res* 171: 105780. https://doi.org/10.1016/j.phrs.2021.105780
5. Cavuoto P, Fenech MF (2012) A review of methionine dependency and the role of methionine restriction in cancer growth control and life-span extension. *Cancer Treat Rev* 38: 726−736. https://doi.org/10.1016/j.ctrv.2012.01.004
6. Zgheib R, Battaglia-Hsu SF, Hergalant S, et al. (2019) Folate can promote the methionine-dependent reprogramming of glioblastoma cells towards pluripotency. *Cell Death Dis* 10: 596. https://doi.org/10.1038/s41419-019-1836-2
7. Zhang S, Cheng C, Lin Z, et al. (2022) The global burden and associated factors of ovarian cancer in 1990–2019: findings from the Global Burden of Disease Study 2019. *BMC Public Health* 22: 1455. https://doi.org/10.1186/s12889-022-13861-y
8. Murali R, Balasubramaniam V, Srinivas S, et al. (2023) Deregulated metabolic pathways in ovarian cancer: cause and consequence. *Metabolites* 13: 560. https://doi.org/10.3390/metabo13040560
9. Younesian S, Mohammadi MH, Younesian O, et al. (2024) DNA methylation in human diseases. *Heliyon* 10: e32366. https://doi.org/10.1016/j.heliyon.2024.e32366
10. Ehrlich M (2019) DNA hypermethylation in disease: mechanisms and clinical relevance. *Epigenetics* 14: 1141–1163. https://doi.org/10.1080/15592294.2019.1638701
11. Landgraf BJ, McCarthy EL, Booker SJ (2016) Radical S-adenosylmethionine enzymes in human health and disease. *Annu Rev Biochem* 85: 485−514. https://doi.org/10.1146/annurev-biochem-060713-035504
12. Wanders D, Hobson K, Ji X (2020) Methionine restriction and cancer biology. *Nutrients* 12: 684. https://doi.org/10.3390/nu12030684
13. Abdelraof M, Selim MH, Elsoud MM, et al. (2019). Statistically optimized production of extracellular l-methionine γ-lyase by *Streptomyces* Sp. DMMMH60 and evaluation of purified enzyme in sub-culturing cell lines. *Biocatal Agr Biotechnol* 18: 101074. https://doi.org/10.1016/j.bcab.2019.101074
14. Al-Zahrani NH, Bukhari KA (2019) Molecular identification, gene detection, and improving L-methioninase production of *Serratia* SP. isolate. *Pharmacophore* 10: 14–25.

15. Aldawood AS, Al-Ezzy RM (2024) Cytotoxicity of l-methioninase purified from clinical isolates of *pseudomonas* species in cancer cell lines. *Al-Rafidain J Med Sci* 6: 46−49. https://doi.org/10.54133/ajms.v6i1.405
16. Kholmurodov BO, Jurayev RS (2024) Quantitative analysis of vitamins and amino acids in alhagi mauro-rum plant extract. *Eng Proc* 67: 32. https://doi.org/10.3390/engproc2024067032
17. Javia BM, Gadhvi MS, Vyas SJ, et al. (2024) A review on L-methioninase in cancer therapy: precision targeting, advancements and diverse applications for a promising future. *Int J Biol Macromol* 265: 130997. https://doi.org/10.1016/j.ijbiomac.2024.130997
18. Thivat E, Durando X, Demidem A, et al. (2007) A methionine-free diet associated with nitrosourea treatment down-regulates methylguanine-DNA methyl transferase activity in patients with metastatic cancer. *Anticancer Res* 27: 2779−2783.
19. Locasale JW, Melman T, Song S, et al. (2012) Metabolomics of human cerebrospinal fluid identifies signatures of malignant glioma. *Mol Cell Proteom* 11: M111.014688. https://doi.org/10.1074/mcp.M111.014688
20. Kokkinakis DM, Brickner AG, Kirkwood JM, et al. (2006) Mitotic arrest, apoptosis, and sensitization to chemotherapy of melanomas by methionine deprivation stress. *Mol Cancer Res* 4: 575−589. https://doi.org/10.1158/1541-7786.mcr-05-0240
21. Lu X (2019) The role of large neutral amino acid transporter (LAT1) in cancer. *Curr Cancer Drug Tar* 19: 863−876. https://doi.org/10.2174/1568009619666190802135714
22. Cunningham A, Erdem A, Alshamleh I, et al. (2022) Dietary methionine starvation impairs acute myeloid leukemia progression. *Blood* 140: 2037−2052. https://doi.org/10.1182/blood.2022017575
23. Xin L, Yang WF, Zhang HT, et al. (2018) The mechanism study of lentiviral vector carrying methioninase enhances the sensitivity of drug-resistant gastric cancer cells to Cisplatin. *Brit J Cancer* 118: 1189−1199. https://doi.org/10.1038/s41416-018-0043-8
24. Kubota Y, Sasaki M, Han Q, et al. (2024) Efficacy of recombinant methioninase on late-stage patient cancer in the histoculture drug response assay (HDRA) as a potential functional biomarker of sensitivity to methionine-restriction therapy in the clinic. *Cancer Diagn Progn* 4: 239. https://doi.org/10.21873/cdp.10314
25. Strekalova E, Malin D, Hoelper D, et al. (2018) Abstract LB-247: targeting methionine metabolism to eradicate cancer stem cells. *Cancer Res* 78: LB-247. https://doi.org/10.1158/1538-7445.AM2018-LB-247
26. Liu Y, Guo J, Cheng H, et al. (2024) Methionine restriction diets: unravelling biological mechanisms and enhancing brain health. *Trends Food Sci Tech* 2024: 104532. https://doi.org/10.1016/j.tifs.2024.104532
27. Abdulabbas HS, Al-Mawlah YH (2023) Effect of Rs5746136 genotypes on SOD activity and biomarkers levels in breast cancer patients. *AIMS Biophys* 10: 1−11. https://doi.org/0.3934/biophy.2023001